LA-UR-95-1020

Conf-950127--1

Los Alamos National Laboratory is operated by the University of California for the United States Department of Energy under contract W-7405-ENG-36

Title: Recent Results from NA44 and a Review of HBT

Author(s): Barbara V. Jacak, for the NA44 Collaboration

Submitted to: Quark Matter '95: Proceedings of the Eleventh International Conference on Ultra-Relativistic Nucleus-Nucleus Collisions, Monterey, CA, January 9–13, 1995

LosAlamos Los Alamos National Laboratory
Los Alamos, New Mexico 87545

Form No. 836 R4
ST NO 2629 5/81

DISCLAIMER

Portions of this document may be illegible in electronic image products. Images are produced from the best available original document.

Recent Results from NA44 and a Review of HBT

Barbara V. Jacak, for the NA44 Collaboration

H. Boggild[a], J. Boissevain[b], M. Cherney[c], G. Ditore[d], J. Dodd[e], B. Erazmus[f], S. Esumi[g], C. Fabjan[d], D.E. Fields[b], D. Ferenc[h], A. Franz[d], J. Gaardhoje[a], K. Hansen[a], O. Hansen[a], D. Hardtke[i], B. Holzer[d], T. Humanic[i], B.V. Jacak[b], R. Jayanti[i], H. Kalechofsky[j], T. Kobayashi[k], R. Kvatadze[l], P. Lautridou[f], Y. Lee[m], M. Leltchouk[d], B. Lorstad[n], T. Ljubicic[h], N. Maeda[g], N. Matsumoto[g], A. Medvedev[e], A. Miyabayashi[n], M. Murray[o], S. Nishimura[g], E. Noteboom[c], G. Paic[f], S. Pandey[i], F. Piuz[d], J. Pluta[f], M. Potekhin[e], V. Polychronakos, G. Poulard[d], A. Rahmani[f], J. Rieubland[d], A. Sakaguchi[g], K. Shigaki[q], J. Simon-Gillo[b], J. Schmidt-Sorenson[a], W. Sondheim[b], M. Spegel[d], T. Sugitate[g], J.P. Sullivan[b], Y. Sumi[g], H. van Hecke[b], G. Vilkelis[i], W. Willis[e], K. Wolf[o], N. Xu[b]

[a]Niels Bohr Institute, DK-2100 Copenhagen, Denmark
[b]Los Alamos National Laboratory, Los Alamos, NM 87545, USA
[c]Creighton University, Omaha, NE, USA
[d]CERN, CH-1211 Geneva 23, Switzerland
[e]Columbia University, New York, NY 10027, USA
[f]Nuclear Physics Laboratory of Nantes, 44072 Nantes, France
[g]Hiroshima University, Higashi-Hiroshima 724, Japan
[h]Rudjer Boskovic Institute, Zagreb, Croatia
[i]Ohio State University, Columbus, Ohio 43210, USA
[j]Now at University of Geneva, Geneva, CH-1211, Switzerland
[k]Riken Linac Laboratory, Riken, Saitama 351-01, Japan
[l]Visitor from Tbilisi State University, Tbilisi, Rep. Of Georgia
[m]Now at GSI Laboratory, Darmstadt, D-6100, Germany
[n]University of Lund, S-22362 Lund, Sweden
[o]Texas A&M University, College Station, TX 77843, USA
[p]Brookhaven National Laboratory, Upton, NY 11973, USA
[q]University of Tokyo, Tokyo 113, Japan

1. INTRODUCTION

High energy heavy ion collisions provide the opportunity to create hadronic matter at high energy density and study its properties. In order to do this, we must characterize the collisions, ascertain the size and density of the hot system in the central region of the nucleus-nucleus system, and determine the energy density achieved. Furthermore, we need to determine whether or not the system approaches equilibrium so thermodynamic descriptions may be used. One of the experimental tools available is the study of two-particle correlations to map the

space-time extent of the system when the hadrons decouple [1]. Other observables include the flow of energy and charged particles transverse to the beam and the rapidity distribution of protons to indicate the amount of stopping and randomization of the incoming energy. The transverse mass distributions of hadrons reflect the temperature of the system at freezeout and effects of radial expansion [2]. The production ratios of different particles are related to the extent of chemical equilibrium reached in the collision and subsequent evolution of the hadron gas. The NA44 Experiment at CERN can address all of these observables, though here we focus mainly on correlation measurements.

Kaons and pions are emitted rather late in the evolution of a heavy ion collision, at the time of "freezeout" when the hadrons cease to interact. Their correlations reflect the space-time evolution of the later part of the collision. In addition to characterizing the collision, correlations can signal a phase transition as they measure the duration of hadronization and particle emission, which should be long in both a first- or second-order phase transition [1]. Furthermore, correlation measurements offer an important tool to help disentangle effects of expansion from the freezeout temperature reflected in the single particle spectra [3].

In these proceedings, we describe the analysis methods employed to determine the shape of the hadronic source from high statistics data in section II. Section III describes the NA44 experiment at the CERN SPS, and shows results of both two-particle correlations and single-particle distributions. In section IV, global trends of the radius parameters measured by a number of different experiments are shown. A number of issues are raised by the data, and we describe the use of an event generator to guide interpretation of the experimental results in section V. The event generator allows a comparison of the information extracted from the correlation functions with the actual spatial distribution of the particles at freezeout in the simulation. Section VI extracts information about the collision dynamics from the data. If single-particle distributions and correlation functions from the event generator agree with the data, a detailed study of the collision evolution in the event generator can help separate effects of collision dynamics from the measurement of the hadronic source size at freezeout. The last section gives conclusions that may be drawn from the body of data measured in high energy heavy ion collisions.

2. MODERN METHODS OF CORRELATION ANALYSIS

Two-particle correlation functions are measured to study the space-time evolution of the hadronic (i.e., later) part of the collision. In high energy heavy ion collisions, two-boson correlations, namely pions or kaons, are measured and the analysis follows the general philosophy pioneered by Hanbury-Brown and Twiss [4].

The lifetime of the source and its transverse expansion may be strongly influenced by the presence of a phase transition; thus the correlation studies may provide a possible plasma formation signal in addition to characterizing the

collision. The measured correlation function represents the Fourier transform of the particle distribution inside the emitting source if

(1) the particles are emitted incoherently,
(2) they do not arise predominantly from resonance decays,
(3) they do not interact with each other or the rest of the system
(4) there are no kinematic correlations.

We will comment on the validity of these assumptions, and note how interpretation of the results depends on them.

Correlation functions are customarily fit assuming a Gaussian-distributed source, though the distribution may be expected to have a more complex shape [5,6]. High-statistics data allow multi-dimensional fits. These do not require the unrealistic assumption of a spherical source, are more sensitive to the collision dynamics, and less influenced by relativistic effects than correlations analyzed in the four-momentum difference, q_{inv}, of the two particles. q_{inv} is an average over all directions of the pairs within the acceptance of the experiment.

The experimental correlation functions are constructed from the ratio of the two-particle cross section to the product of the two single particle cross sections, evaluated by taking particles from different events. These are usually fit with the function [1]:

$$C_2 = C\left(q_{t_o}, q_{t_s}, q_l\right) = D\left[1 + \exp\left(-q_{t_o}^2 R_{t_0}^2 - q_{t_s}^2 R_{t_s}^2 - q_l^2 R_l^2\right)\right] . \qquad (1)$$

The relative momentum vector is decomposed into a longitudinal component, q_l, parallel to the beam axis, and two transverse components, q_{t_0} and q_{t_s}, which are perpendicular to the beam axis. q_{t_0} is along the momentum sum of the two particles, and q_{t_s} is perpendicular to it. Being parallel to the velocities of the particles, q_{t_0} is sensitive to the lifetime of the source [1]. This can be extracted from the fit parameters by

$$R_{t_0}^2 = R_{t_s}^2 + (\beta\Delta\tau)^2 , \qquad (2)$$

where β is the velocity of the particle pair, $\Delta\tau$ is the difference in emission time between them and reflects the duration of freezeout. The R parameters are related to the Gaussian sizes of the source in the specified directions. The strength of the correlation is given by the λ parameter, sometimes called the chaoticity parameter.

Different experiments analyze correlations in somewhat different reference frames. NA44 [7,8] analyzes in the frame in which the particle pair momentum sum along the beam direction is zero, the LCMS, or Longitudinal Center of Mass, frame. This frame couples the lifetime information solely to q_{t_0}. NA35 [9,10] and E802/E859/E866 [11–13] analyze in the nucleon-nucleon center of mass frame, which is similar (but not identical) to the LCMS near mid-rapidity. This reference frame is near the rest frame of the particle source.

There are also other systematic differences in the results reported by different experiments. NA35 includes a factor of 1/2 in the Gaussian fit function, which

yields radius parameters larger by $\sqrt{2}$ than those from other experiments. In order to compare the fit parameters to physically meaningful sizes, it is necessary to convert them to either an r.m.s. radius or to the equivalent hard sphere radius for comparison with the projectile size. The r.m.s. radius from a three dimensional correlation function analysis is given by

$$\langle r^2 \rangle^{1/2} \{3d\} = \sqrt{\left(R_x^2 + R_y^2 + R_z^2\right)} \,. \tag{3}$$

For a spherical source, $R_x = R_y = R_z$, the r.m.s. radius is $\sqrt{3}R$. To determine the hard sphere radius, one must use

$$\langle r^2 \rangle \{3d\} = \int_0^{R_{t_s}} \left(r^2 r^2 \, dr\right) \Big/ \int_0^{R_{t_s}} \left(r^2 \, dr\right) = 3/5 \, R_{t_s}^2 \,. \tag{4}$$

Consequently, the value to compare with a projectile size calculated using $1.2 A^{1/3}$ is $\sqrt{(3/5)R_{t_s}}$. It is important to remember the factor of $\sqrt{5}$ difference between the fit parameters and nuclear radii.

3. NA44 EXPERIMENT AND RESULTS

NA44 is a second-generation experiment, and consists of a focusing spectrometer optimized for the study of identified single and two-particle distributions at midrapidity. Excellent particle identification limits contamination to the 1% level. Since it is a focusing spectrometer, the acceptance for pairs of particles with small momentum difference is optimized, allowing small statistical uncertainties in the region of the signal from Bose-Einstein correlations.

The layout of NA44 is shown in Fig. 1. There are three dipole magnets (D1, D2, D3) and three quadrupoles (Q1, Q2, Q3); the first two dipoles select the momentum and the last one is used for momentum calibration. Only one charge state can be detected at one time. The momentum range selected by the spectrometer covers a band of ± 20% around the nominal setting. The angular coverage is approximately –0.3 to 4.5 degrees in the horizontal and ± 0.3 degrees in the vertical plane.

The spectrometer uses three highly segmented scintillator hodoscopes (H1, H2, H3), for tracking and time-of-flight measurements in the p and S collision data. For Pb + Pb collisions, the tracking elements are H2 and H3, along with a pad chamber at the exit of Q3 and two strip chambers.

The beam rate and time-of-flight start are determined with a Čerenkov beam counter (CX) for heavy ion beams, and a forward scintillator (T0) for proton beams. The intrinsic time resolution of the Čerenkov beam counter is approximately 35 ps [14]. The forward scintillator is used as a triggering device in both cases, to signal either minimum bias or central collisions via the pulse height. A silicon pad multiplicity detector is used to measure the charged particle distribution with 2π acceptance in the range $1.5 < \eta < 3.3$. Čerenkov

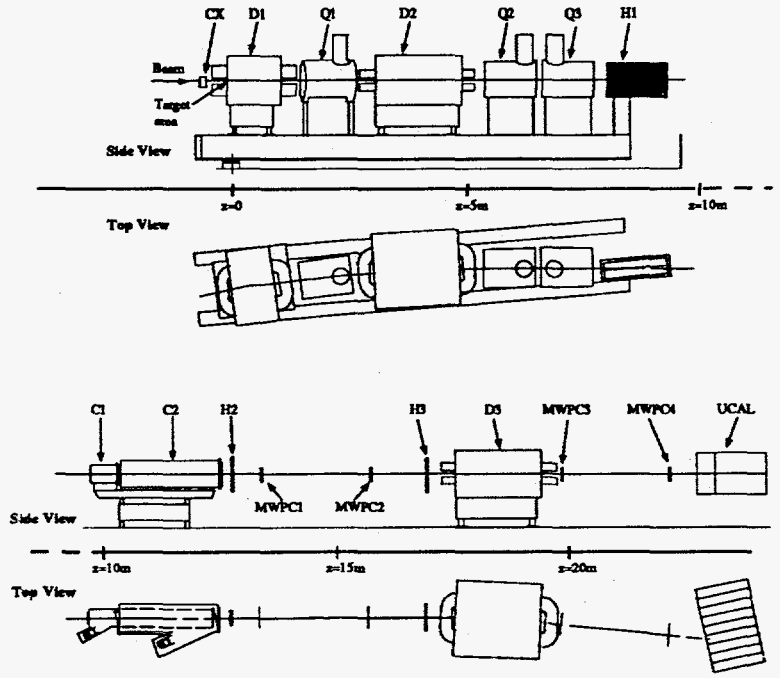

Fig. 1. Layout of the NA44 experiment.

detectors (C1, C2) are used to provide a kaon or proton trigger by vetoing events containing electrons, muons, or pions in the spectrometer. Muons from kaon decays after the Čerenkov counters are vetoed if they are above the Čerenkov momentum threshold 1.9 GeV/c, or if they do not form straight line trajectories.

The spectrometer acceptance is $3.2 < y < 4.2$ and $0 < p_t < 0.6$ GeV/c for low p_t pions, $2.5 < y < 3.1$ and $0.3 < p_t < 0.8$ GeV/c for high p_t pions, and $2.7 < y < 3.3$ and $0 < p_t < 0.7$ GeV/c for the kaon setting. Protons are measured in 0.3 units of rapidity, centered about $y = 2.8$, with $p_t = 0$–800 MeV/c.

Figure 2 shows the correlation function of pion pairs in 200 GeV/A S + Pb collisions, analyzed in three dimensions [15]. The shape of the correlation function is nearly but not quite consistent with a Gaussian-distributed pion source. Study of this shape difference using an event generator has shown that it arises from resonance decays. Decays of η and ω, in particular, contribute pions that affect the correlation function in the region of the Bose-Einstein signal and modify the extracted R parameters.

Results on correlations of K^+ and K^- pairs have long been awaited for two reasons: the relative freedom from resonance decay products and the opportunity to compare K^+, which has a small nucleon-scattering cross section, with K^-, which has a considerably larger cross section. K^+ and K^- correlation functions measured by NA44 in 200 GeV/A S + Pb collisions and analyzed in two dimensions, q_t and q_l, are shown in Fig. 3; the comparison is limited by the K^- pair statistics. The results for K^+ and K^- are similar, indicating that the different interaction cross section with nucleons is not important in the central region at SPS energies. This is confirmed by our measurement of the ratio $p/\pi^+ = 0.0.25$ [16]. $K\pi$ scattering dominates, and is similar for K^+ and K^-.

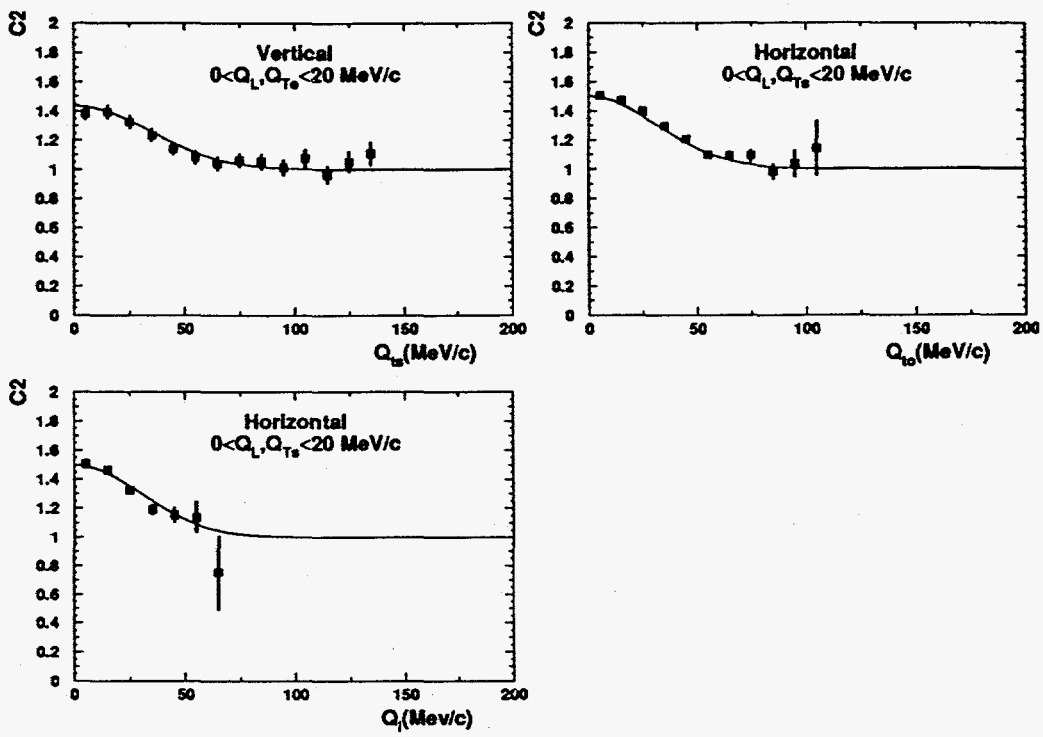

Fig. 2. Correlation function of positive pions from S + Pb collisions, analyzed in three dimensions, from NA44 [15].

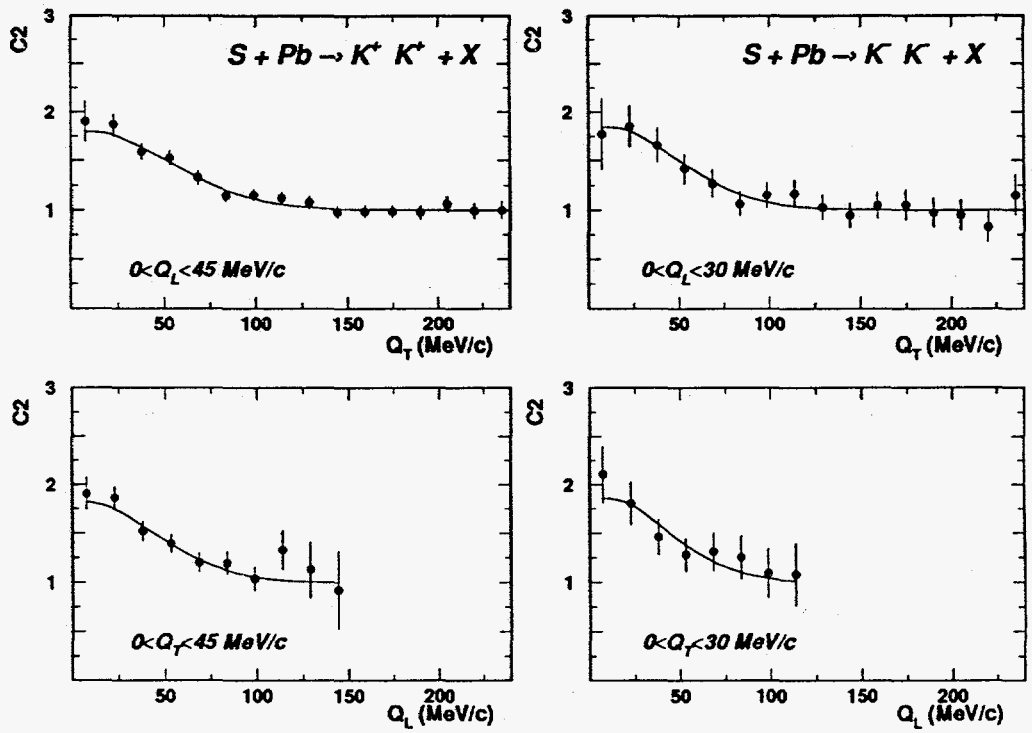

Fig. 3. K^+ and K^- correlation functions measured by NA44 in S + Pb collisions [7].

Table 1 summarizes the R parameters extracted by NA44 from three-dimensional analysis of pion and kaon correlations in S + Pb and p + Pb collisions. Several trends are obvious. The R parameters for pions are larger than those of the kaons, as was also observed by E802 at lower collision energy [12], and the λ parameter is larger. Both trends may be expected from the lesser production of kaons than pions by decays of long-lived resonances. Such decay products are formed after freezeout, and represent an uncorrelated background to the Bose-Einstein signal, hence the decrease in the λ parameter. The R parameters in S + Pb collisions are larger than those in p + Pb collisions, as might be expected. R_{t_s} in S + Pb collisions is larger than the projectile size. This implies a significant expansion of the system before freezeout.

Table 1
R parameters measured by NA44 for S + Pb and p + Pb collisions [7,8].

	R_{t_s}	R_{t_o}	R_l	λ
$S + Pb \rightarrow \pi^+$	4.15 ± 0.20	4.02 ± 0.14	4.73 ± 0.26	0.56 ± 0.02
$p + Pb \rightarrow \pi^+$	2.00 ± 0.25	1.92 ± 0.13	2.34 ± 0.36	0.41 ± 0.02
$S + Pb \rightarrow K^+$	2.55 ± 0.20	2.77 ± 0.12	3.02 ± 0.20	0.82 ± 0.04
$p + Pb \rightarrow K^+$	1.22 ± 0.76	1.53 ± 0.17	2.40 ± 0.30	0.70 ± 0.07

The table also shows that $R_{t_o} \approx R_{t_s} \approx R_l$, particularly for S + Pb. In fact, the data show $R_{t_o} \approx R_{t_s} \approx R_l \propto 1/\sqrt{m_t}$ for all mesons, with $m_t^2 = p_t^2 + m^2$. This behavior is illustrated in Fig. 4 [3], which shows pion and kaon data from S + Pb collisions, plotted as a function of $\sqrt{m_t}$; the highest m_t point is the kaon point. The dotted line indicates $2/\sqrt{m_t}$. This dependence on $\sqrt{m_t}$ is notable because a simple hydrodynamical model of a cylindrically symmetric expanding source predicts just such a dependence [17]. The common behavior with $\sqrt{m_t}$ of pions and kaons suggests equilibration and supports the applicability of hydrodynamics. The expansion creates correlations between a particle's position and momentum, negating one of the assumptions made in fitting correlation functions and relating the fit parameters to the source size.

The dependence on $\sqrt{m_t}$ can be predicted from a cylindrically symmetric three-dimensional expanding source [17]. The velocity gradient together with the freeze-out temperature generate a length scale in all three dimensions. If the source length scales are much larger than this, the three measured R parameters become equal (in the LCMS frame) and show a dependence on $1/\sqrt{m_t}$. The RQMD model [18], discussed in detail below, also shows this dependence and agrees with our data. The source also expands in RQMD, driven by the numerous secondary collisions among the particles. We will return to this below.

In November 1994, first lead beams became available at CERN. NA44 collected data on pion and kaon pairs, and single particle distributions. First analysis of correlation functions in two dimensions already shows trends, though detailed studies of the acceptance corrections are still under way. As in S + Pb,

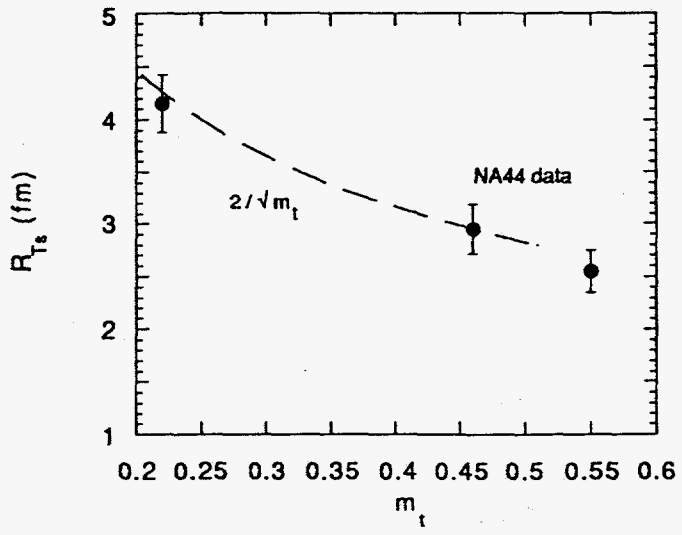

Fig. 4. m_t dependence of the R_{t_s} parameter. Data are from NA44 [3,15]; the lower two m_t points are from pions and the highest from kaons.

correlation functions in Pb + Pb collisions show decreasing R parameters with increasing m_t. The R parameters in Pb + Pb are, however, larger than in S + Pb, particularly R_l. This may be expected as the projectile is larger, but it should be noted that the values of the R parameters are larger than the projectile for both S and for Pb beams.

The single particle distributions in Pb + Pb collisions are exponential in m_t. This is observed for pions, kaons, and protons, and the inverse slopes are summarized in Table 2. It should be noted that the pion slope is fitted for $m_t >$ 150 MeV, to avoid any possible electron contamination. In Pb + Pb collisions, the K^+ and K^- spectra look rather similar. Both are well fit with a single exponential, and they have the same inverse slope within statistical errors. These data are discussed further in the contribution from J. Dodd in these proceedings.

Table 2
Preliminary inverse slopes of single particle m_t spectra in Pb + Pb collisions. Systematic errors are estimated at 15%.

π^+	K^+	p
145 ± 8 MeV	206 ± 4 MeV	250 ± 7 MeV

In the motivation for three-dimensional analysis, we discussed the possibility of measuring the lifetime of the particle source. Equation (2) should hold as long as the particles are not strongly influenced by expansion of the source. Consequently, this equation should be applied at low m_t, where the expansion effects are smallest. NA44, and other experiments such as NA35 at the SPS [9], and

E859/E866 at the AGS [13], find values of R_{t_o} and R_{t_s} that do not differ significantly. Where an emission can be calculated at all, times of 2–3 fm/c with large error bars result. The RQMD event generator yields longer emission times. However, it is not clear how significant this apparent difference between the data and RQMD is, as the experimental determinations of the source lifetime suffer from statistical problems and the influence of collision dynamics.

4. GLOBAL TRENDS OF RADIUS PARAMETERS

The results presented above from NA44 can be compared with measurements by NA35 and WA80 at the SPS, and with results from E859/E866 and E814 at the AGS. We may further determine the bombarding energy dependence of the R parameters by comparing these to results from the Bevalac.

There are differences in the R parameters between experiments, even where NA44 and NA35 cover nominally the same rapidity range. There is, of course, the trivial factor of $\sqrt{2}$ between NA44 and NA35 due to the fit function, but the parameters differ beyond this [8,9]. RQMD events filtered with experimental acceptance agree well with both experiments [8,10], and show that the differences are acceptance effects [19]. Though both experiments are at midrapidity, the shape of the acceptance in y and p_t differs; the NA44 acceptance is considerably more complicated.

Table 3 shows the R parameters for π^+ and K^+ pairs in 14.6 GeV/nucleon Si + Au collisions, measured by E859 [13] and analyzed in three dimensions. E859 uses the same fit function as NA44, so the parameters may be compared. As stated above, the transverse R parameters from kaons are smaller than those from pions, and the λ parameter is larger. The values of the parameters are somewhat smaller than those measured at SPS energy.

Table 3
R parameters in 14.6 GeV/nucleon Si + Au collisions, measured by E859 [13].

	R_{t_s}	R_{t_o}	R_l	λ
π^+	2.95 ± 0.19	2.77 ± 0.13	2.75 ± 0.15	0.65 ± 0.02
K^+	2.09 ± 0.20	2.07 ± 0.16	1.71 ± 0.14	0.83 ± 0.08

WA80 [20] has measured two-pion and two-proton correlations in the target rapidity region, $-1 < y < 1$, at the SPS. The R parameter from proton correlation functions is extracted using a very different procedure from the one above, as protons are fermions. The resulting R parameter shows a clear dependence on $A^{1/3}$ for p-, O-, and S-induced collisions on various targets [20], and so reflects the target geometry.

For pion correlation functions, WA80 fits a one-dimensional Gaussian source. The resulting R parameters do not show a simple dependence on the size of the

target nucleus. The interpretation of this finding is still under study. However, the pions detected in the target rapidity region likely contain contributions both from the central rapidity source, which is characterized by the experiments looking in midrapidity, as well as from the excited target remnant. The resulting R parameters are likely to be sensitive both to the collision geometry (i.e., impact parameter) and the pion multiplicity in the central region.

The differences observed between NA44 and NA35 underscore the caution required when comparing results from different experiments, even when the same fit function is used. Keeping in mind that the systematic errors on such a comparison are necessarily large, some global trends may be extracted from Figs. 5 and 6. These figures show the dependence of R_t, the transverse radius parameter in a two dimensional analysis of pion correlation functions, at Bevalac, AGS, and SPS energies. The Bevalac data are taken from the Streamer Chamber [21] and the Janus Spectrometer [22,23], AGS from E859/E866 [13], and SPS from NA35 [9] and NA44.

Figure 5 shows the dependence of R_t on the projectile mass. A clear difference in R_t is visible when comparing proton and heavy ion projectiles. However, the dependence on A_{proj} is minimal among the heavy ion projectiles. In Fig. 6, the dependence of R_t on $\sqrt{s}$ of the collision is illustrated; Fig. 6(a) shows asymmetric systems, and 6(b) shows symmetric systems. No $\sqrt{s}$ dependence is visible in Fig. 6(a). Figure 6(b) separates light ($A < 100$) and heavy ($A > 100$) symmetric systems, and shows a $\sqrt{s}$ dependence only for the heavy systems. These include La + La at the Bevalac [22], Au + Au at the AGS [13], and the preliminary Pb + Pb result from NA44. The NA44 result is shown as an upper limit, as the acceptance corrections are known to increase the R parameter values. For heavy systems, R_t increases markedly with $\sqrt{s}$, whereas it is nearly independent for smaller systems both symmetric and asymmetric. These results, along with the observations of p_t and m_t dependence of the R parameters discussed above, emphasize the caution that must be used before interpreting the R parameters as geometrical sizes of the collision zone.

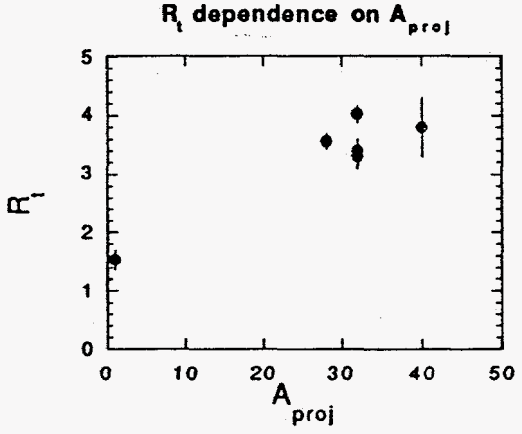

Fig. 5. Dependence of R_t from two-dimensional analysis of π on correlations on the size of the projectile. Data are from Bevalac, AGS, and SPS as stated in the text.

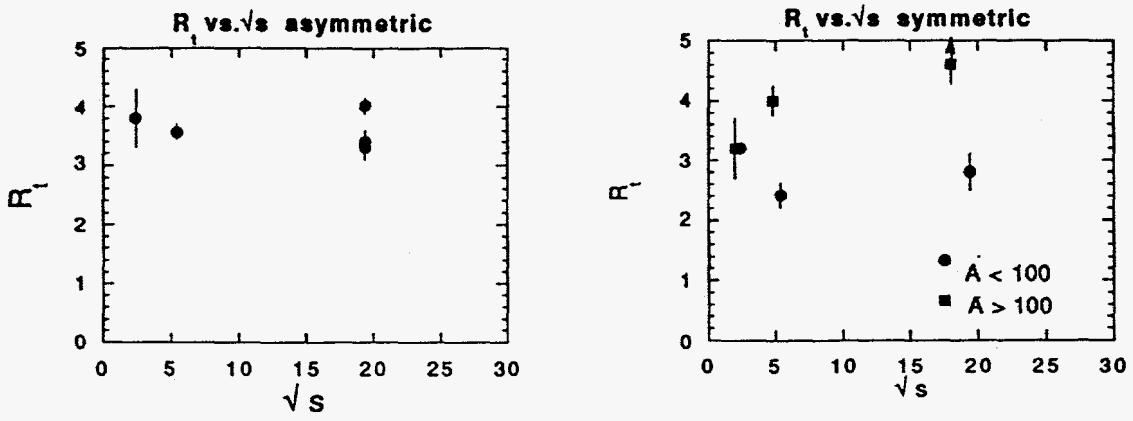

Fig. 6. Dependence of R_t on the $\sqrt{s}$ of the collision. Data are from Bevalac, AGS, and SPS as stated in the text. (a) shows asymmetric projectile-target systems and (b) symmetric systems.

5. MODEL COMPARISONS

The data raise a number of questions. In order to properly interpret the fit parameters, we need to know what determines the shape of the correlation functions and what resonance decay effects are important. Furthermore, we need to explore the sensitivity of the fit parameters to the collision dynamics. A tool to guide the interpretation of the correlation fit parameters is comparison with an event generator incorporating the collision dynamics, particle production, hadron rescattering, and resonance formation and decay. Many experiments currently use the RQMD event generator [18], which gives good agreement with single-particle distributions.

To study correlation functions, the model is used to generate the phase-space coordinates of hadrons at the time they suffer their last strong interaction. Using the freezeout position and momentum of pairs of randomly selected particles, a two-particle symmetrized wave function is calculated and used to add Bose-Einstein correlations [5,6]. The particles are first subjected to the experimental acceptance cuts, and the resulting correlation functions are fit in the same way as the data. This procedure has been adopted by most of the experiments.

The event generator tool allows investigation of the relationship between the fit parameters and the source size we wish to measure. We begin by comparing the calculated correlation function with the particle distributions at freezeout. Such a comparison is shown in Fig. 7 for S + Pb collisions at 200 GeV/nucleon [6]. The top half shows the pion (solid lines) and kaon (dotted lines) distributions at freezeout along the beam direction, transverse to the beam direction, and in time. The kaon distributions are narrower than the pions, in agreement with the data.

The lower section of the figure shows correlation functions calculated several ways from RQMD events. They are plotted in the variable which corresponds most closely to the directions in the top part of the figure, along the beam direction (q_{par} or q_l), transverse to the beam ($q_{t_{side}}$), and $q_{t_{out}}$, which is a

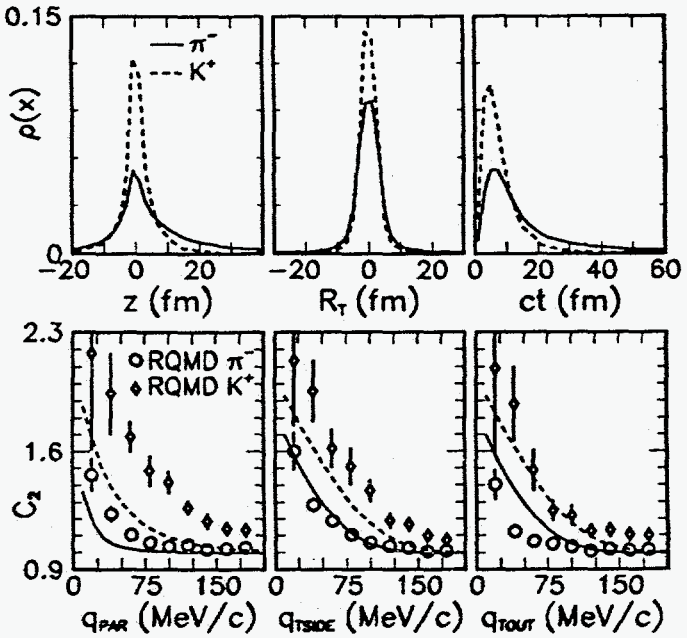

Fig. 7. Comparison of position distributions at freezeout and calculated correlation functions, both from RQMD events [6]. The events are filtered with the NA35 epxerimental acceptance to generate the correlation functions.

combination of the time and transverse size. The solid and dashed lines indicate the Fourier transform of the position distributions in the top part of the figure. The points show the calculated RQMD correlation functions using the NA35 experimental acceptance. Comparison of the curves allows evaluation of how closely the measured correlation functions actually reflect the source sizes. It is evident that the agreement is far from perfect. Along the beam direction, there are significant effects of Lorentz extension of the measurement reference frame with respect to the source frame [26], along with the position-momentum correlations caused by the longitudinal expansion [8,17]. Analysis in $q_{t_{side}}$ most closely approximates the transverse size of the source, but is also subject to error from position-momentum correlations induced by transverse expansion. This correlation increases with increasing particle transverse mass, and is reflected in the larger deviation of the calculated correlation function from the kaon Fourier transform. The position-momentum correlation increases the difference between K and π fit parameters, and causes the observed m_t dependence. The correlation functions in $q_{t_{out}}$ should not agree directly with the time distribution as they also include the source transverse size. These effects may be untangled, however, by using the information from the event generator to scale the R parameters extracted from the data.

It is, of course, important to remember that a significant fraction of the observed pions arises from the decay of long-lived resonances. RQMD shows that more than half of the low p_t pions are from such resonances [6], while the contribution to the observed kaons is much smaller. These decay products can be seen as tails on the otherwise Gaussian distribution of pion positions at freezeout in the upper middle panel of Fig. 7.

The m_t dependences of the R parameters observed by NA44 are quite well reproduced by RQMD [3]. NA35 finds that RQMD agrees reasonably well with the p_t dependence of R_{t_s} for S + S, S + Ag, and S + Au collisions, though R_{t_o} is somewhat overpredicted [10]. E814 at the AGS finds good agreement of RQMD with a one-dimensional analysis of pion pairs from 14.6 GeV/A Si + Pb collisions [24]. E859/866 compare multidimensional analyses and find that RQMD reproduces π and K pairs from 14.6 GeV/A Si + Au very well [13]; the ARC event generator developed for AGS energy collisions [25] gives reasonable agreement, but somewhat underpredicts the R parameters for pions [13]. From these comparisons and the fact that RQMD predicts radial expansion of the source, the E814 collaboration concludes that significant expansion takes place at the AGS. The suggestion that the m_t and p_t dependence of the R parameters at SPS energy is caused by expansion is confirmed by the RQMD comparisons.

6. COLLISION DYNAMICS

In the sections above there has been much discussion of radial expansion in heavy ion collisions. We will examine this further in this section.

It has long been known that a hydrodynamical expansion in the longitudinal direction may be expected in high-energy collisions. This is known as the "boost invariant expansion" [27] and should lead to a 1/cosh(y) dependence of the longitudinal R parameter. Such behavior has been reported by NA35 [9].

If the collision also satisfies the requirements that the particles decouple instantaneously at a time τ_f, and the particle spectrum is thermal with a temperature T_f (global thermalization is not necessary, just local), then the following equation should hold:

$$R = \sqrt{(T_f/m_t)}\ \tau_f/\cosh(y)\ , \tag{5}$$

where y is the source rapidity in the observer rest frame. Such behavior was predicted for R_l, but the $\sqrt{m_t}$ dependence is also observed for R_{t_s} and R_{t_o}. In this case,

$$R = \sqrt{(T_f/m_t)}\ \tau_f\ . \tag{6}$$

The scale of the measured m_t dependence, i.e., 2.0 from NA44 measurements in S + Pb collisions, should determine τ_f, and through it the expansion velocity. Though extracting a velocity from τ_f requires an assumption about the shape of the freezeout surface, a simple shape assumption for this is reasonable. Such an

analysis represents an exciting opportunity for an independent determination of the expansion velocity.

Figure 8 shows the positions and momenta at freezeout of pions in 200 GeV/A S + Pb collisions simulated by RQMD [19]. The direction transverse to the beam, labeled y, is used. A clear correlation is visible — particles with positive p_y are more likely to be found at positive y. The effect of this correlation is also seen in the widths of the y position distributions from RQMD events. They decrease with increasing p_t, similarly to the R_{t_s} parameter extracted from both data and RQMD correlation functions. This correlation results from the radial expansion.

It should be noted that correlations between position and momentum arising from expansion were predicted some time ago. Padula, Gyulassy, and Gavin cautioned experiments that it would affect the R parameters extracted from the data [28]. An analysis similar to the one using RQMD events described above was made on events from the ARC generator by Nayak and Zajc [26], who also found narrowing of the widths of the transverse position distributions with increasing p_t. RQMD as well as ARC shows the position-momentum correlations typical of radial expansion at AGS energy; a figure similar to Fig. 8 was shown by the E814 collaboration [24].

In fact, even at Bevalac energy, there are indications for the presence of some radial expansion. In 1986, Beavis et al. measured the momentum dependence of the R parameter from a one-dimensional analysis of π correlations in 1.8 GeV/A Ar + Pb collisions [21]. They found that R decreases with increasing magnitude of the average pion pair momentum. This was interpreted as evidence for expansion of the system before freezeout.

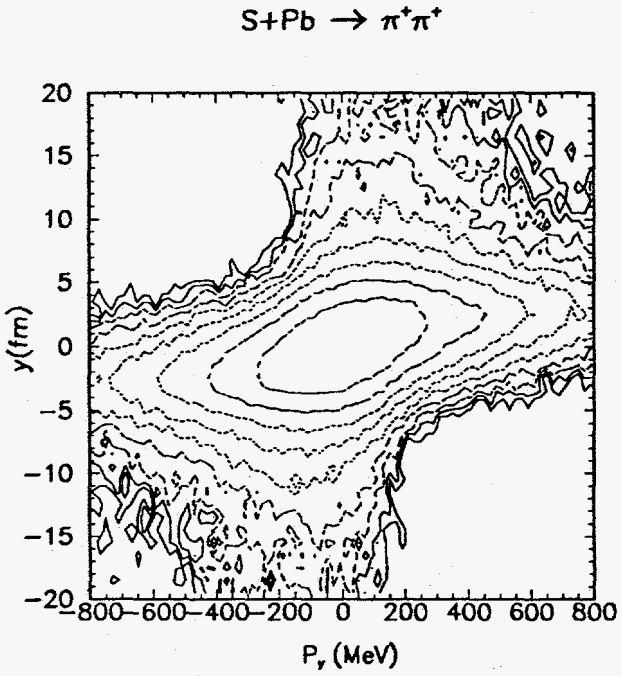

Fig. 8. The transverse momentum vs. transverse position of pions at freezeout in RQMD S + Pb events. A clear correlation is visible.

As discussed above, RQMD shows considerable transverse expansion of the source prior to freezeout at both AGS and SPS energies. This expansion is driven by the numerous collisions among the produced particles. We have investigated it quantitatively, by looking at the time evolution of the average particle transverse velocities at midrapidity in RQMD events [29]. It is found that a significant outward, or radial, flow velocity is developed. Velocities as high as β = 0.4–0.5 are predicted by RQMD both at SPS and AGS energies. Construction of the stress tensors from the RQMD events indicates hydrodynamic behavior and significant flow in these collisions [29].

It is logical to ask whether the single particle distributions, traditionally used to look for flow effects, are consistent with such expansion velocities. We have analyzed the single particle distributions measured by NA44 in S + Pb collisions using an expanding source in local equilibrium. This analysis follows the prescription developed by Schnedermann et al. [30] and was applied to single-particle distributions at AGS energy [21]. A velocity profile $\beta_r = \beta_r^{max} (r/2)^2$ was used in this calculation.

Figure 9 shows that a freezeout temperature, T_f, of 140 MeV and maximum transverse expansion velocity β = 0.42 reproduce the π, K, p, and d distributions quite well. The T_f and β parameters are not uniquely determined by the single-particle data; other combinations can also describe the spectra. However, the m_t dependence of the R parameters offers a potent new tool in unraveling T_f and β in a model-independent way. The problem is underconstrained by either single- or two-particle distribution alone, but should be constrained by the simultaneous use of both.

7. CONCLUSIONS

We have presented an overview of current methods of analyzing Bose-Einstein correlation data, and compared the results from NA44 to those from other experiments. We have shown that the R parameters from fitting the data do not directly yield the source size, but the measurements are very useful nevertheless. Interpretation of the parameters from fitting correlation functions is complicated by resonance decays and experimental acceptance effects, as well as by the collision dynamics. However, the use of event generators allows making a connection between these parameters and the geometrical size of the emitting source.

The measurements indicate significant radial expansion in heavy ion collisions. This expansion creates a correlation between the position and momentum of the detected particles, and causes the R parameters to reflect only part of the source. The $\sqrt{m_t}$ dependence offers a way to measure the expansion velocity experimentally. Comparison to models also yields an estimate of the amount of expansion. Armed with the expansion velocity from correlation measurements, the freezeout temperature can be extracted from the single-particle spectra. Particles at low $\sqrt{m_t}$ should be less affected by the expansion, so will be more sensitive to the source lifetime. However, there are substantial contributions from resonance decays, so care is required to extract a geometrical source size even from these particles.

As discussed above, RQMD shows considerable transverse expansion of the source prior to freezeout at both AGS and SPS energies. This expansion is driven by the numerous collisions among the produced particles. We have investigated it quantitatively, by looking at the time evolution of the average particle transverse velocities at midrapidity in RQMD events [29]. It is found that a significant outward, or radial, flow velocity is developed. Velocities as high as β = 0.4–0.5 are predicted by RQMD both at SPS and AGS energies. Construction of the stress tensors from the RQMD events indicates hydrodynamic behavior and significant flow in these collisions [29].

It is logical to ask whether the single particle distributions, traditionally used to look for flow effects, are consistent with such expansion velocities. We have analyzed the single particle distributions measured by NA44 in S + Pb collisions using an expanding source in local equilibrium. This analysis follows the prescription developed by Schnedermann et al. [30] and was applied to single-particle distributions at AGS energy [21]. A velocity profile $\beta_r = \beta_r^{max} (r/2)^2$ was used in this calculation.

Figure 9 shows that a freezeout temperature, T_f, of 140 MeV and maximum transverse expansion velocity β = 0.42 reproduce the π, K, p, and d distributions

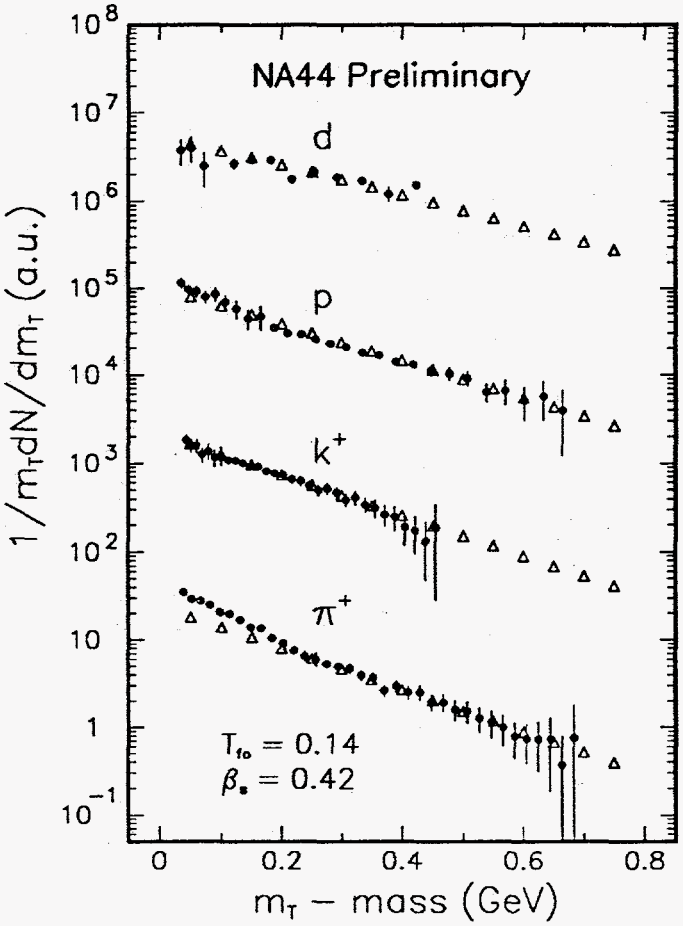

Fig. 9. Single-partlcle m_t distributions for pions, kaons, protons, and deuterons measured by NA44 in S + Pb collisions. The lines indicate a fit with a thermalized, expanding source.

quite well. The T_f and β parameters are not uniquely determined by the single-particle data; other combinations can also describe the spectra. However, the m_t dependence of the R parameters offers a potent new tool in unraveling T_f and β in a model-independent way. The problem is underconstrained by either single- or two-particle distribution alone, but should be constrained by the simultaneous use of both.

7. CONCLUSIONS

We have presented an overview of current methods of analyzing Bose-Einstein correlation data, and compared the results from NA44 to those from other experiments. We have shown that the R parameters from fitting the data do not directly yield the source size, but the measurements are very useful nevertheless. Interpretation of the parameters from fitting correlation functions is complicated by resonance decays and experimental acceptance effects, as well as by the collision dynamics. However, the use of event generators allows making a connection between these parameters and the geometrical size of the emitting source.

The measurements indicate significant radial expansion in heavy ion collisions. This expansion creates a correlation between the position and momentum of the detected particles, and causes the R parameters to reflect only part of the source. The $\sqrt{m_t}$ dependence offers a way to measure the expansion velocity experimentally. Comparison to models also yields an estimate of the amount of expansion. Armed with the expansion velocity from correlation measurements, the freezeout temperature can be extracted from the single-particle spectra. Particles at low $\sqrt{m_t}$ should be less affected by the expansion, so will be more sensitive to the source lifetime. However, there are substantial contributions from resonance decays, so care is required to extract a geometrical source size even from these particles.

REFERENCES

1. S. Pratt, Phys. Rev. D33 (1986) 1314; G. Bertsch and G.E. Brown, Phys. Rev. C40 (1989) 1830.
2. K. S. Lee, U. Heinz, and E. Schnedermann, Z. Phys. C48 (1990) 525.
3. H. Beker et al. (NA44 Collaboration), Phys. Rev. Lett, in press.
4. R. Hanbury-Brown and R. Q. Twiss, Nature 178 (1956) 1046.
5. S. Pratt, T. Csorgo, and J. Zimanyi, Phys. Rev. C42 (1990) 2646.
6. J. Sullivan et al., Phys. Rev. Lett. 70 (1993) 3000.
7. H. Beker et al. (NA44 Collaboration), Z. Phys. C64 (1994) 209.
8. H. Beker et al. (NA44 Collaboration), CERN-PPE/94-119, accepted by Phys. Rev. Lett.
9. Th. Alber et al. (NA35 Collaboration), IKF-HENPG/9-94 (1994).
10. Th. Alber et al. (NA35 Collaboration), submitted to Phys. Rev. Lett. (1994).
11. T. Abbott et al. (E802 Collaboration), Phys. Rev. Lett. 69 (1992) 1030.
12. Y. Akiba et al. (E802 Collaboration), Phys. Rev. Lett. 70 (1993) 1057.

13. V. Cianciolo et al. (E858 collaboration) and F. Videbaek et al. (E866 collaboration), these proceedings.
14. N. Maeda et al., Nucl. Instrum. Methods A346 (1994) 132.
15. H. Boggild et al. (NA44 Collaboration), CERN-PPE/94-177, Phys. Lett, in press.
16. M. Murray et al. (NA44 collaboration), Nucl. Phys. A566 (1994) 515c.
17. T. Csorgo and B. Lorstad, Univ. Lund preprint LUNFD6/9NFF1-7082 (1994); Yu. M. Sinyukov, Nucl. Phys. A566 (1994) 589c.
18. H. Sorge, H. Stoecker and W. Greiner, Ann. Phys. 192 (1989) 266.
19. D.E. Fields et al., LA-UR-95-666 (1995).
20. T. Peitzmann et al. (WA80 collaboration), Proc. of CORINNE II, Nantes, France, June 1994.
21. D. Beavis et al., Phys. Rev. C34 (1986) 757.
22. H. Bossy et al., Phys. Rev. C47 (1993) 1659.
23. A.D. Chacon et al., Phys. Rev. C43 (1991) 2670.
24. J. Barrette et al. (E814 Collaboration), Phys. Lett. B333 (1994) 33.
25. S.H. Kahana, Y. Pang, T. Schlagel, and C.B. Dover, Phys. Rev. C47 (1993) R1356.
26. W.A. Zajc, Proc. of the NATO School on Particle Production in Highly Excited Matter, Il Ciocco, Italy, July 1992, p.435.
27. J.D. Bjorken, Phys. Rev. D27 (1983) 140.
28. S. Padula, M. Gyulassy, and S. Gavin, Nucl. Phys. B329 (1990) 357.
29. N. Xu, G. Baym, D.E. Fields, H. van Hecke, B.V. Jacak, J. Simon-Gillo, J.P. Sullivan, to be published.
30. E. Schnedermann, J. Sollfrank, and U. Heinz, Phys. Rev. C48 (1993) 2462.
31. P. Braun-Munzinger, J. Stachel, H. Wessels, and N. Xu, Phys. Lett. B344 (1995) 43.